ORGANOMETALLICS

pubs.acs.org/Organometallics Article

The Unusual Structural Behavior of Heteroleptic Aryl Copper(I) Thiolato Molecules: Cis vs Trans Structures and London Dispersion Effects

Wenxing Zou, James C. Fettinger, Petra Vasko,* and Philip P. Power*

Cite This: *Organometallics* 2022, 41, 794–801 Read Online

ACCESS | Metrics & More | Article Recommendations | Supporting Information

ABSTRACT: A series of heteroleptic aryl copper(I) thiolato complexes of formula $\{Cu_2(SAr)Mes\}_2$ (Ar = C_6H_3-2,6-(C_6H_2-2,4,6-Me_3)$_2$ (Ar^{Me6}), **1**; C_6H_3-2,6-(C_6H_3-2,6-iPr_2)$_2$ (Ar^{iPr4}), **2**; C_6H_3-2,6-(C_6H_2-2,4,6-iPr_3)$_2$ (Ar^{iPr6}), **3**) and $\{Cu_4(SAr)Mes_3\}$ (Ar = C_6H-2,6-(C_6H_2-2,4,6-iPr_3)$_2$-3,5-iPr_2 (Ar^{iPr8}), **4**) were synthesized by the reactions of the corresponding bulky terphenyl thiols with mesitylcopper(I) with elimination of mesitylene. All complexes were characterized by single crystal X-ray diffraction analysis and spectroscopy (NMR, infrared, and UV−vis). The data for **1**−**3** revealed tetrametallic Cu_4 core structures in which two thiolato or two mesityl ligands bridge the metals. Although **1** and **2** feature the expected conventional alternating thiolato and mesityl bridging patterns, **3** has a previously unknown structural arrangement in which the two thiolato ligands are adjacent to each other. Since complex **3** has a more crowding aryl group on the thiolato ligands, the cis arrangement of the ligands in **3** is sterically counterintuitive and is likely due to London dispersion (LD) energy effects. Complex **4** also has an unusual structural pattern in which only a single thiolato ligand is incorporated in the structure probably for steric reasons. It has a planar trapezoidal Cu_4 core in which three Cu−Cu edges are bridged by the mesityl groups while the remaining Cu−Cu edge is thiolato ligand bridged. Dispersion connected DFT calculations show that **3** has the highest LD effect stabilization arising from the increased numbers of C−H···H−C interactions of the isopropyl ligand substituents.

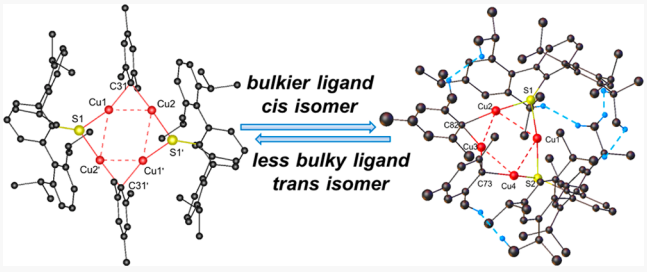

■ INTRODUCTION

Sterically crowding ligands are widely used in inorganic/organometallic chemistry to stabilize compounds with unusual coordination numbers, bonding, and/or oxidation states.[1−5] Their use is predicated on the notion that such ligands repel each other due to their overlapping electron clouds. In effect, there is intrusion of electronic wave functions on each other's space contrary to the Pauli exclusion principle, i.e., Pauli repulsion. However, in addition to this repulsion, there is growing evidence that attractive London dispersion (LD) interactions between the C−H moieties of the hydrocarbyl substituents of the ligands[5−7] can generate unexpected effects and enable the formation of species with unusual structures. Such effects are manifested, for example, in the stable hexaphenylethane derivative $\{C(C_6H_3\text{-}3,5\text{-}^tBu_2)_3\}_2$ of Grimme and Schreiner,[8] the divalent group 14 chalcogenetates,[9] high oxidation state mid- to late transition metal alkyls,[10,11] or in the low coordinate copper(II) amides.[12] In pursuit of further examples of low coordinate copper(II) species, we investigated the use of large terphenyl substituted thiolato ligands where dispersion effects had been noted earlier by Ziegler.[5] The use of the terphenyl thiolato ligands has recently afforded the first dimeric copper(I) thiolato derivatives[13] $\{CuSAr^{iPr4}\}_2$ and $\{CuSAr^{iPr6}\}_2$ from the reaction of the thiol with a mesitylcopper(I)[14] precursor. Upon further investigation we found that adjustment of the ratio of the thiolate ligand to copper yielded unknown types of heteroleptic organo/thiolato copper molecules $\{Cu_2(SAr)Mes\}_2$ (Mes = $-C_6H_2$-2,4,6-Me_3; Ar = $-C_6H_3$-2,6-(C_6H_2-2,4,6-Me_3)$_2$ (Ar^{Me6}), **1**; $-C_6H_3$-2,6-(C_6H_3-2,6-iPr_2)$_2$ (Ar^{iPr4}), **2**; $-C_6H_3$-2,6-(C_6H_2-2,4,6-iPr_3)$_2$ (Ar^{iPr6}), **3**) and $\{Cu_4(SAr)Mes_3\}$ (Ar = C_6H-2,6-(C_6H_2-2,4,6-Me_3)$_2$-3,5-iPr_2 (Ar^{iPr8}), **4**). Whereas **1** and **2** feature the expected alternating thiolato and mesityl ligands in which the pairs of mesityl and thiolato groups appear trans to each other, the more crowded Ar^{iPr6} substituted **3** has a structure in which the mesityl and thiolato groups have mutually cis positions apparently as a result of enhanced ligand dispersion effects. This cis structural arrangement of ligands was unknown in organocopper chemistry featuring Cu_4 core arrays. X-ray crystallographic studies revealed that complexes **1**−**4** display Cu_4 cores but their thiolato ligands were found to have

Received: January 12, 2022
Published: March 8, 2022

Downloaded via UNIV OF CALIFORNIA DAVIS on May 7, 2023 at 20:47:21 (UTC).
See https://pubs.acs.org/sharingguidelines for options on how to legitimately share published articles.

ACS Publications © 2022 American Chemical Society

https://doi.org/10.1021/acs.organomet.2c00018
Organometallics 2022, 41, 794−801

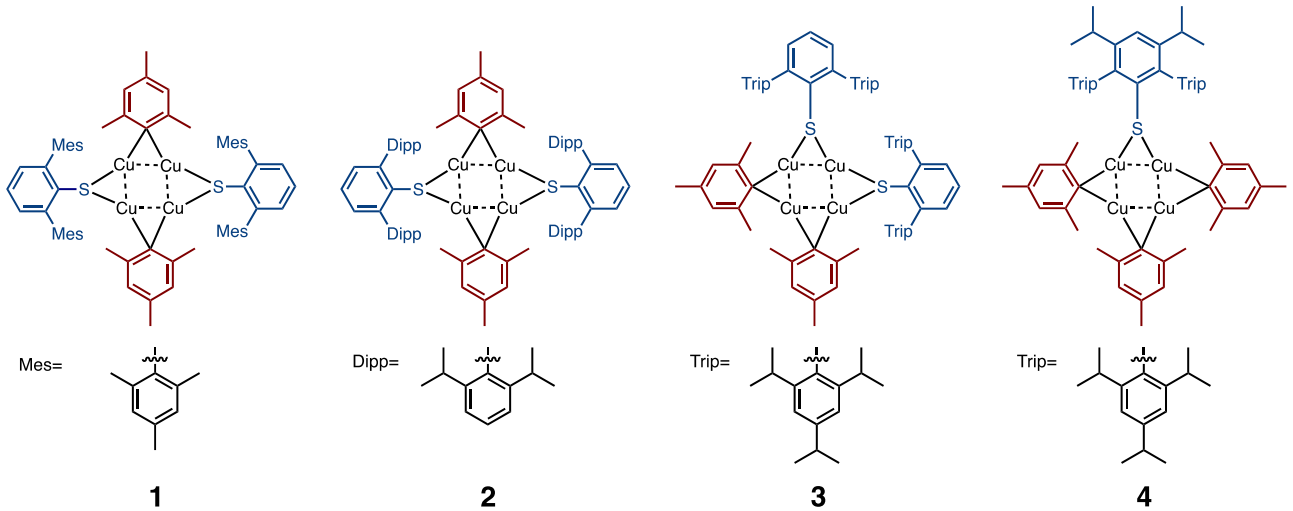

Figure 1. Complexes **1**−**4** with different ligand arrangements.

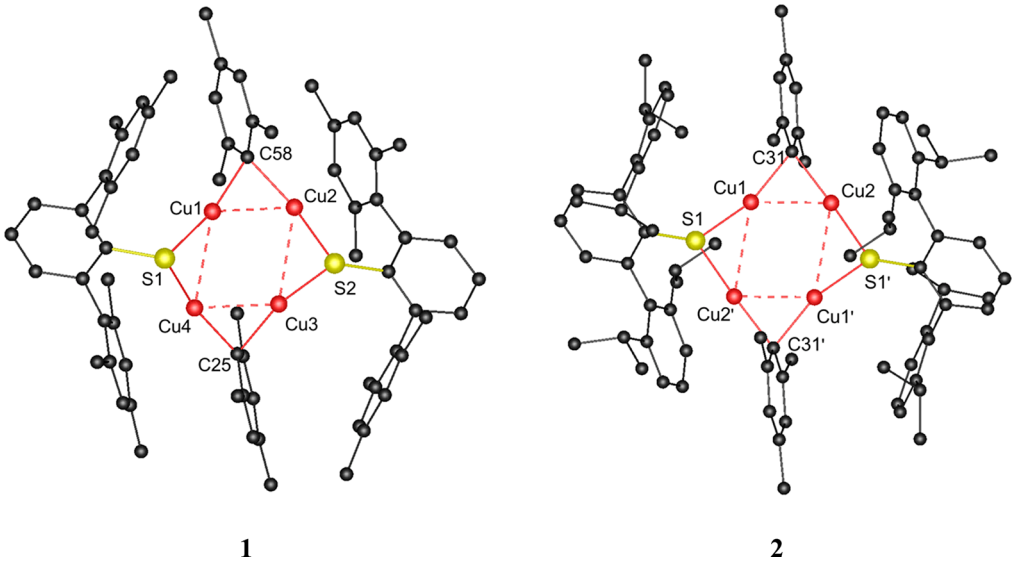

Figure 2. Molecular structures of **1** and **2** with thermal ellipsoids shown at 30% probability. Hydrogen atoms are not shown. Selected lengths (Å) and angles (deg) of **1**: Cu1−Cu2 2.43(5), Cu2−Cu3 2.86(7), Cu3−Cu4 2.43(5), Cu4−Cu1 2.82(7), S1−Cu1 2.16(8), S1−Cu4 2.18(8), C58−Cu1 2.00(2), C58−Cu2 1.99(2), Cu1−Cu2−Cu3 77.97(17), Cu2−Cu3−Cu4 101.86(2), Cu1−C58−Cu2 75.20(8), Cu2−S2−Cu3 80.96(3), and for **2**: Cu1−Cu2 2.45(5), Cu1−Cu2′ 2.92(6), S1−Cu1 2.17(6), S1−Cu2′ 2.16(6), C31−Cu1 2.00(2), C31−Cu2 1.97(18), Cu1−Cu2−Cu1′ 80.58(17), Cu2−Cu1′−Cu2′ 99.42(17), Cu1−C31−Cu2 75.86(7), Cu1−S1−Cu2′ 84.73(2).

different arrangements relative to the Cu_4 core, Thus, whereas **1** and **2** have symmetrical structures and alternating aryl and thiolate ligands (Figure 1), **3** has a unique cis disposition of these ligands. The very large size of the aryl substituents in **4** prevents the incorporation of further thiolato groups.

■ RESULTS AND DISCUSSION

Structures. The reactions of the terphenyl thiols ($HSAr^{Me6}$ for **1**, $HSAr^{iPr4}$ for **2**, $HSAr^{iPr6}$ for **3**, and $HSAr^{iPr8}$ for **4**) and half equivalent of $\{CuMes\}_4$ in THF at 80 °C for 2 days (in toluene at 110 °C, 4 days for **4**) afforded the aryl copper terphenyl thiolates **1**−**4**. The structures of the heteroleptic aryl/thiolato copper derivatives **1** and **2** have little precedent but they are related to previously reported heteroleptic tetracopper species $\{Cu_2RindBr\}_2$ (Rind = rigid fused-ring s-hydrindacenyl skeleton)[15] and $\{LAl(R)OCu{\cdot}MesCu\}_2$ (L= $HC[C(Me)N(Dipp)]_2$, R = Me or Et).[16] The compound **1** (Figure 2, left) displays a Cu_4 core array arranged in a nonplanar parallelogram in which the metals are bridged by the C_{ipso} atoms of the mesityls or thiolato ligand sulfur atoms in an alternating manner. The two sulfur atoms are located on the same side of the Cu_4 core. The S atoms have pyramidalized coordination in which the sum of the angles at S = 302.22(14)°. The Cu−Cu distances bridged by the thiolato groups are 2.82(7) and 2.86(7) Å, whereas those bridged by the mesityl ligands are ca. 0.4 Å shorter at 2.43(5) and 2.43(5) Å. The latter pair of distances are greater than the sum of the covalent radii (2.24 Å)[17] of two Cu atoms but lie within the sum of the van der Waals radii (2.8 Å),[18] suggesting either no covalent Cu−Cu bonding or weak van der Waals interactions. The lengths of Cu−S bonds range from 2.16(11) to 2.18(9) Å, which are similar to those in other copper thiolates.[19] Likewise, the structure of complex **2** (Figure 2, right) is similar to that of **1**, but it has a center of symmetry in which the planar, rectangular Cu_4 core is also coplanar with C_{ipso} atoms C31 and

https://doi.org/10.1021/acs.organomet.2c00018
Organometallics 2022, 41, 794−801

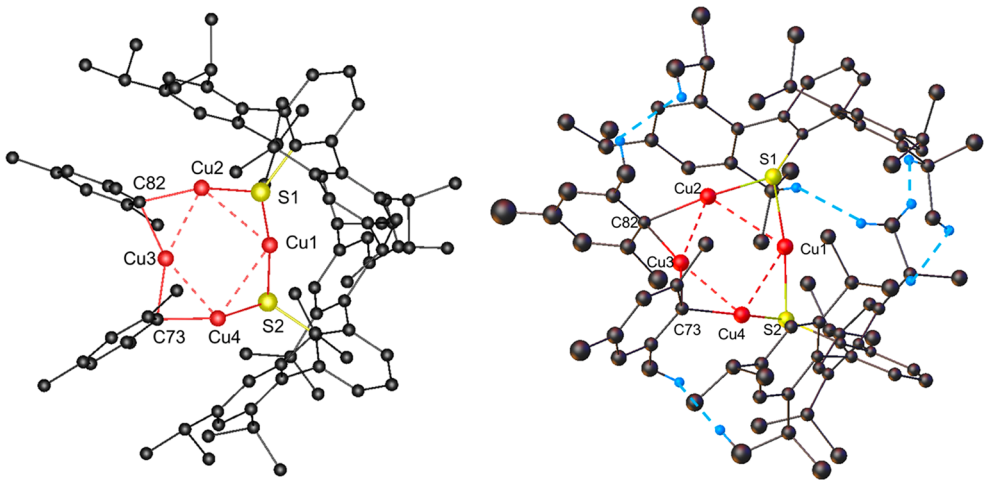

Figure 3. Molecular structure of **3** with thermal ellipsoids shown at 30% probability (left). Selected interatomic distances (Å) and angles (deg): Cu1−Cu2 2.73(5), Cu1−Cu4 2.76(5), Cu2−Cu3 2.42(5), Cu3−Cu4 2.42(5), S2−Cu1 2.17(6), S2−Cu4 2.20(6), C82−Cu2 2.01(2) C82−Cu3 2.00(2), Cu1−Cu2−Cu3 77.21(16), Cu2−Cu3−Cu4 111.87(19), Cu3−Cu4−Cu1 76.74(15), Cu4−Cu1−Cu2 94.10(16), Cu1−S2−Cu4 78.02(2), Cu3−C73−Cu4 74.60(8). Some interligand H−H contacts across the Cu_4 core within the sum of their van der Waals radii (ca. 2.4 Å) are indicated with dashed blue lines (right). All other hydrogens are not shown.

C31′ of the mesityl groups. The two pyramidally coordinated S atoms of the thiolato ligands are located on the opposite side of the Cu_4 plane with a distance of 0.76(8) Å between the S atom and extended Cu_4 core that generates an interplanar angle of 24.91(18)°. As before, the separation of the Cu atoms bridged by the thiolates (2.92(6) Å) is much greater than the separation between copper atoms bridged by the mesityl groups (2.45(5) Å).

The combination of the thiol $HSAr^{iPr6}$ and $\{CuMes\}_4$ in THF with stirring at 80 °C for 2 days gave a pale yellow solution which, upon removal of the solvent under reduced pressure and recrystallization from toluene, yielded complex **3** in 16% yield. Complex **3** incorporates two bulkier thiolato ligands, but its structure displays a cis arrangement of the ligands in which the S atoms of thiolato groups bridge the two adjacent Cu−Cu edges. In the solid state, **3** was observed to have a previously unknown and sterically counterintuitive cis arrangement of the ligands (shown in Figure 3, left). The Cu1−Cu2 and the adjacent Cu1−Cu3 edges are bridged by the S atoms of thiolato groups while the Cu2−Cu4 and the adjacent Cu3−Cu4 edges are bridged by the C_{ipso} atoms of mesityl groups. The Cu−Cu distances spanned by the thiolato ligands are more than ca. 0.3 Å longer than the Cu−Cu distances bridged by the mesityl groups (2.42(5) Å), which is consistent with the distances in **1** and **2** above. Complex **3** also has several close interligand H−H contacts across the Cu_4 core within the sum of their van der Waals radii (ca. 2.4 Å) arising from the isopropyl groups of the thiolato and mesityl substituents (indicated with dashed blue lines in Figure 3, right), suggesting an LD interaction between thiolato and mesityl CH_3 groups. In contrast, no close interligand H−H contacts were observed in the molecular structures of either **1** or **2**, suggesting the sterically counterintuitive structure of **3** is a consequence of enhanced LD effects caused by increased number of isopropyl substituents.

We also investigated the reaction of the extremely bulky Ar^{iPr8} substituted thiol $HSAr^{iPr8}$ and $\{CuMes\}_4$ under similar conditions to those used for **3**, expecting to isolate a further example of a cis-substituted aryl thiolato copper isomer, i.e., $\{Cu_2(SAr^{iPr8})Mes\}_2$, with a structure analogous to that of **3**. The reaction of $HSAr^{iPr8}$ and $\{CuMes\}_4$ in toluene at 110 °C for 4 days gave a yellow solution, from which some colorless crystals were isolated after 4−5 days' storage in a ca. 5 °C refrigerator. However, crystallographic and spectroscopic results showed that the complex incorporated only a single thiolato ligand, which resulted in an unusual, trapezoidal Cu_4 core array in which three Cu−Cu edges are bridged by the mesityls, while one Cu−Cu edge is bridged by the thiolato ligand (Figure 4).

As depicted in Figure 4, complex **4** has an unusual trapezoid-shaped Cu_4 core with bridging by three mesityl groups and a single thiolato ligand. The essentially planar Cu_4 core lies parallel to the central ring of the thiolato ligand with a vertical distance of 2.11(17) Å (see side view in Figure 4); the mesityl group that bridges Cu2 and Cu2′ is essentially perpendicular to the Cu_4 core plane. The sulfur atom S1 is located on the opposite side of the central ring of the thiolato ligand relative to the Cu_4 core (a distance of 0.058(12) Å between the sulfur and the extended central ring). C32 atom is located on the same side of the Cu_4 plane relative to the sulfur atom with a distance between S1 and extended Cu_4 plane of 0.97(9) Å; C23 and C23′ atoms lie on the other side (a distance between C23 and extended Cu_4 plane of 0.74(3) Å). The molecule is symmetric with respect to a mirror plane that is perpendicular to the Cu_4 plane and contains the C1−S1 single bond. The Cu1−Cu2 and Cu2−Cu2′ distances are slightly different (by ca. 0.08(5) Å). The Cu1−Cu2 distance is 2.45(5) Å, which is in the normal range for aryl copper species.[14,20] However, the Cu2−Cu2′ distance was determined to be 2.37(8) Å, which is at the shorter end of the range for Cu(I) thiolates,[13,21] aryl copper complexes[14,20] or even copper amides.[22−24] The Cu1−Cu1′ distance is 3.21(8) Å, which is considerably greater than the sum of the van der Waals radii (2.8 Å),[17] suggesting no significant interaction between these two copper centers.

Spectroscopy. The ^1H NMR spectrum of complex **1** is relatively simple and well resolved, showing two singlet signals at 1.98 (12H) and 1.85 (24H) ppm in C_6D_6 attributable to the protons of the methyl groups of the thiolato ligands. There are also two singlet signals centered at 2.28 (12H) and 2.21 (6H) ppm, which can be assigned to the methyl hydrogens of the

https://doi.org/10.1021/acs.organomet.2c00018
Organometallics 2022, 41, 794−801

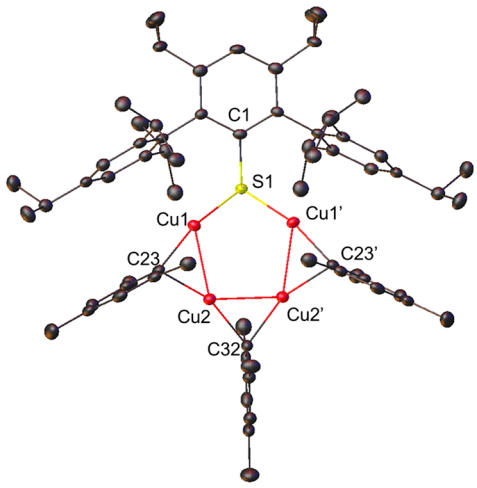

top view

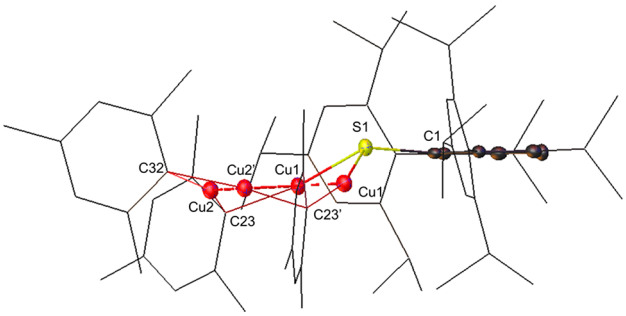

side view (ligands are shown as wire frames)

Figure 4. Top view and side view of the molecular structures of **4** with thermal ellipsoids shown at 30% probability (top view). Hydrogen atoms are not shown. Selected distances (Å) and angles (deg): Cu1−Cu2 2.45(5), Cu2−Cu2′ 2.37(8), Cu1−Cu1′ 3.21(8) S1−Cu1 2.17(6), C1−S1 1.78(3), Cu1−C23 1.98(2), Cu2−C32 1.99(2), Cu1−Cu2−Cu2′ 99.91(13), Cu1−S1−Cu1′ 95.43(4), Cu1−C23−Cu2 76.31(7), Cu2−C32−Cu2′ 73.14(10).

copper mesityl substituents. The ^{1}H NMR spectrum of complex **2** displays two singlets at 1.20 and 1.00 ppm in the aliphatic region for the methyl groups of the isopropyls of the thiolato ligands, each integrating to 24 hydrogens, and the hydrogens of the mesityl groups are observed as 2.33 and 2.29 ppm. In contrast, complex **3** displays a rather complicated ^{1}H NMR spectrum, which is expected due to the greater degree of magnetic inequivalence caused by the lower symmetry of this molecule. Each isopropyl group has a unique chemical environment, which yields unique chemical shift values making it close to impossible to distinguish them by 1D ^{1}H NMR alone. The ^{1}H NMR spectrum of **4** has two sets of singlets centered at 2.63/2.51 and 1.99/1.76 ppm, respectively, corresponding to para and ortho methyls of the mesityl groups. The spectrum also shows three broadened signals (2.97, 2.54, and 2.41 ppm) expected for the methine hydrogens of isopropyls of the terphenyl thiol. The signals for methyl groups of the isopropyls resonate at 1.77, 1.23, and 1.08 ppm, which are comparable to those of complexes **2** and **3**. The UV−vis spectra of complexes **1**−**4** show broad absorption bands in the range of 273 to 303 nm with the molar extinction coefficient in the range of 1700 to 3000 M^{-1} cm^{-1}, featuring a charge transfer process which is also seen in some related species.[13,25]

Computational Studies. To investigate the bonding in the copper species, the structures of compounds **2** and **3** were optimized using density functional theory (DFT) at the PBE1PBE/Def2-TZVP level of theory with and without empirical dispersion correction (GD3BJ) (see SI, Table S2). Inspection of the optimized bond parameters (Table S2 in SI) reveals that the calculated structures are generally in good agreement with those experimentally observed. The dispersion corrected structures show slightly shorter Cu−Cu distances than those measured in the solid state, but this could be accounted for by the solid-state packing effects. In contrast, the optimizations conducted without a dispersion correction returned gas phase structures with slightly underestimated bond interactions.

Then, the hypothetical structures of cis-**2** and trans-**3** molecules were optimized and the energies of the two isomers were compared (Table 1). The results show that for both compounds **2** and **3** the cis isomer is more stable than the trans isomer. In the case of **2**, however, the Gibbs free energy difference is only 0.2 kJ·mol^{-1} in favor of the cis-isomer, for **3** the energy difference is more substantial, amounting to 15.8 kJ·mol^{-1}. The experimentally obtained isomer **2** is most likely stabilized by solid state effects, which cannot be reproduced by these gas phase calculations.

The thermodynamic data for the dissociation reaction of **2**/**3** → 2 MesCu and 2 TerphSCu fragments were investigated. The data are summarized in Table 2. Without the dispersion effects, the Gibbs free binding energies are 336 and 320 kJ·mol^{-1} for **2** and **3**, respectively.

However, when the dispersion correction is applied, the ΔG value is increased to 549 (for **2**) and 562 (for **3**) kJ·mol^{-1}. These data clearly suggest that dispersion effects play a significant role in the energy of the association of **2** and **3**. This is further corroborated by an energy decomposition analysis (EDA) which confirms that ca. 25% (**2**) and 28% (**3**) of the overall bonding energy can be attributed to dispersion (Figure 5).

Table 1. Calculated Energies (in a.u.) and the Energy Difference (in kJ·mol^{-1}) of the 2 and 3 Cis- and Trans-Isomers

	2_{cis} PBE1PBE-D3	2_{trans} PBE1PBE-D3	3_{cis} PBE1PBE-D3	3_{trans} PBE1PBE-D3
E (a.u.)	−10383.77692	−10383.774290	−10854.820530	−10854.81715
H (a.u.)	−10383.77598	−10383.773346	−10854.819586	−10854.81621
G (a.u.)	−10384.00867	−10383.008598	−10855.092833	−10855.0868
$\Delta E_{cis-trans}$ (kJ·mol^{-1})	−6.9		−8.9	
$\Delta H_{cis-trans}$ (kJ·mol^{-1})	−6.9		−8.9	
$\Delta G_{cis-trans}$ (kJ·mol^{-1})	−0.2		−15.8	

https://doi.org/10.1021/acs.organomet.2c00018
Organometallics 2022, 41, 794−801

Table 2. Energies for the Dissociation Reaction 2/3 → 2 TerphSCu + 2 MesCu (kJ·mol^{-1}) with/without LD Effects

	2	2	3	3
	PBE1PBE-D3	PBE1PBE	PBE1PBE-D3	PBE1PBE
ΔE	740	508	759	502
ΔH	747	515	767	510
ΔG	549	336	562	320

■ CONCLUSION

Four new mixed-ligand copper(I) thiolato compounds were synthesized by the treatment of large terphenyl thiols with mesitylcopper(I). These species have rare Cu_4 core arrays that are bridged by thiolato and organic groups and display a counterintuitive structural arrangement in the case of **3**. Dispersion forces are shown to be a significant factor in the molecular structures of the compounds, which is evidenced by structural and theoretical studies.

■ EXPERIMENTAL SECTION

General Considerations. All manipulations were carried out under anaerobic and anhydrous conditions by using Schlenk techniques or in a Vacuum Atmospheres OMNI-Lab drybox under an atmosphere of dry argon or nitrogen. Solvents were dried by the method of Grubbs[26] and co-workers, stored over potassium or sodium, and then degassed by the freeze−pump−thaw method. All physical measurements were made under strictly anaerobic and anhydrous conditions. The NMR spectra were recorded on a Varian Inova 600 MHz spectrometer, and the ^{1}H NMR spectra were referenced to the residual solvent signals in deuterated benzene, while the ^{13}C NMR spectra were referenced to the residual solvent signals in deuterated THF. IR spectra were recorded as Nujol mulls between CsI plates on a PerkinElmer 1430 spectrometer. UV−vis spectra were recorded as dilute hexane solutions in 3.5 mL quartz cuvettes using an Olis 17 modernized Cary 14 UV−vis−near-IR spectrophotometer or an HP 8452 diode-array spectrophotometer. The terphenyl thiols HSAr^{Me6}, HSAr^{iPr4}, HSAr^{iPr6},[27] and mesitylcopper(I)[14] were prepared via literature methods. Unless otherwise stated, all materials were obtained from commercial sources and used as received.

The syntheses of complexes **1**−**4** are depicted in Figures 6−9.

{Cu$_2$(SAr^{Me6})Mes}$_2$ (1). Solid terphenyl thiol HSAr^{Me6} (0.346 g, 1 mmol) was combined with {CuMes}$_4$ (0.364 g, 0.5 mmol), and ca. 60 mL of THF was added. The solution was heated at 80 °C for 2 days, yielding a pale yellow color. The solvent was then evaporated under reduced pressure to dryness, and the pale yellow residue was extracted with ca. 50 mL of hexane. The solution was filtered through Celite and concentrated to ca. 15 mL under reduced pressure until the formation of small colorless crystals was observed. The solution was stored in a ca. −18 °C freezer for 4 days to yield 0.287 g (24%) of **1** as colorless crystals which were suitable for X-ray crystallography. mp 198−201 °C. ^{1}H NMR (600 MHz, benzene-d_6) δ 7.11 (s, 1H), 6.82 (t, J = 7.2 Hz, 2H), 6.65 (d, J = 1.0 Hz, 2H), 6.64 (d, J = 1.0 Hz, 2H), 6.61 (s, 4H), 6.58 (s, 7H), 2.28 (s, 12H), 2.21 (s, 6H), 1.98 (s, 12H), 1.85 (s, 24H). ^{13}C NMR (150 MHz, benzene-d_6) δ 155.96, 143.29, 139.72, 139.25, 137.12, 136.20, 134.71, 129.30, 128.84, 128.16, 125.49, 125.33, 29.02, 21.21, 21.03, 20.08. UV−vis λ/nm (ε/M^{-1} cm^{-1}) 303 (1700). IR (Nujol; $\tilde{\nu}$/cm^{-1}) 1659w, 1590w, 1562w, 1455s, 1370s, 1258w, 1048w, 841m, 792m, 769w, 737m, 719w, 705w, 571w.

{Cu$_2$(SAr^{iPr4})Mes}$_2$ (2). The synthesis of **2** was accomplished in a similar manner to that of **1** with the use of the terphenyl thiol HSAr^{iPr4} (0.43 g, 1 mmol) and {CuMes}$_4$ (0.364 g, 0.5 mmol) in ca. 60 mL of THF, yielding 0.31 g (23%) of colorless crystals which were suitable for X-ray crystallographic studies. mp decomposed at 190 °C. ^{1}H NMR (600 MHz, benzene-d_6) δ 6.97−6.92 (m, 4H), 6.90 (d, J = 6.7 Hz, 8H), 6.88- 6.83 (m, 6H), 6.71 (s, 4H), 2.73 (m, J = 7.0 Hz, 8H), 2.33 (s, 6H), 2.29 (s, 12H), 1.20 (d, J = 6.9 Hz, 24H), 1.00 (d, J = 6.8 Hz, 24H). ^{13}C NMR (150 MHz, benzene-d_6) δ 156.17, 145.03, 142.55, 140.68, 139.96, 137.24, 132.73, 129.62, 129.60, 126.36, 126.34, 123.04, 30.74, 30.66, 30.11, 24.32, 23.76, 23.73. UV−vis λ/nm (ε/M^{-1} cm^{-1}) 279 (3000). IR (Nujol; $\tilde{\nu}$/cm^{-1}) 1930w, 1584w, 1569w, 1458s, 1371s, 1350m, 1319w, 1275w, 1255w, 1097w, 1050w, 1035m, 929w, 838s, 810m, 791s, 782s, 751s, 742s, 693w, 595w, 566w, 543w, 525w, 462w, 350w.

{Cu$_2$(SAr^{iPr6})Mes}$_2$ (3). The terphenyl thiol HSAr^{iPr6} (0.514 g, 1 mmol), {CuMes}$_4$ (0.364 g, 0.5 mmol) and ca. 60 mL of THF were combined in a Schlenk tube, and the solution was allowed to stir at 80 °C for 2 days. The solvent was removed under reduced pressure, and the residue was extracted with ca. 50 mL of toluene, the resulting solution was filtered through Celite and the filtrate was concentrated to ca. 10 mL under reduced pressure and stored at room temperature for 4 days, yielded 0.24 g (16%) colorless crystals which were suitable for X-ray crystallography. mp 227−231 °C. ^{1}H NMR (600 MHz, benzene-d_6) δ 7.26 (d, J = 13.0 Hz, 3H), 7.11−7.03 (m, 3H), 6.96 (dd, J = 14.8, 7.5 Hz, 3H), 6.76−6.64 (m, 4H), 6.54 (s, 2H), 6.36 (d, J = 18.9 Hz, 3H), 3.14 (q, J = 7.0 Hz, 2H), 2.95 (m, J = 19.8, 6.8 Hz, 5H), 2.89−2.64 (m, 3H), 2.61−2.53 (m, 2H), 2.52−2.32 (m, 8H), 2.26 (s, 5H), 2.08 (d, J = 13.4 Hz, 1H), 2.05 (s, 2H), 1.83 (s, 5H), 1.61 (d, J = 6.8 Hz, 5H), 1.47−1.24 (m, 24H), 1.23 (d, J = 6.9 Hz, 2H), 1.18−1.09 (m, 15H), 1.05 (d, J = 7.0 Hz, 6H), 1.01 (d, J = 6.9 Hz, 6H), 0.97 (d, J = 6.9 Hz, 6H), 0.72 (d, J = 6.8 Hz, 5H). ^{13}C NMR (150 MHz, benzene-d_6) δ 153.69, 153.02, 147.52, 147.42, 147.37, 145.57, 144.88, 142.78, 139.25, 138.04, 137.97, 137.65, 134.96, 130.66, 130.43, 128.92, 127.93, 124.09, 123.71, 121.52, 121.41, 120.98, 34.63, 32.56, 31.68, 31.01, 30.67, 30.64, 30.32, 28.82, 26.15, 25.74, 25.14, 24.98, 24.81, 24.79, 24.44, 24.08, 23.66, 23.25, 23.03, 22.19, 20.92. UV−vis λ/nm (ε/M^{-1} cm^{-1}) 273 (2900). IR (Nujol; $\tilde{\nu}$/cm^{-1}) 1600m, 1589w, 1560w, 1455s, 1375s, 1355m, 1310w, 1255w, 1164w, 1096w, 936w, 872m, 843m, 796m, 761w, 741m, 723m, 688w, 645w, 518w, 459w.

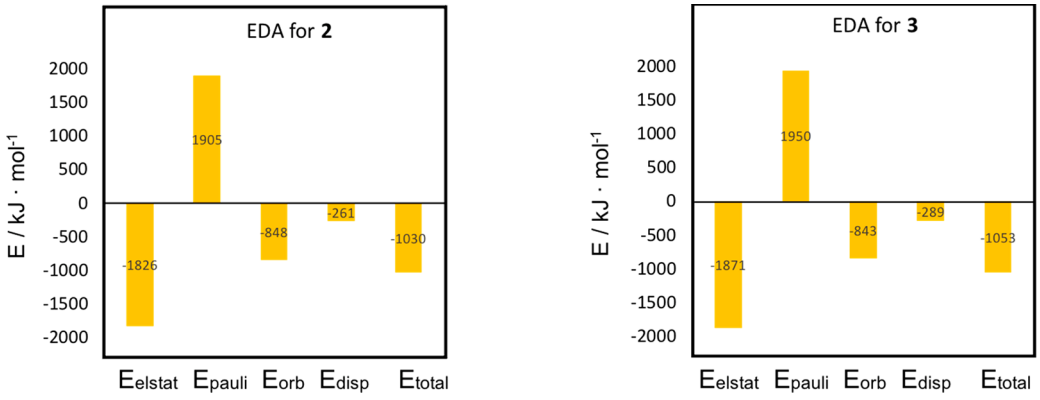

Figure 5. Summary of energy decomposition analysis (EDA) results for **2** and **3** (kJ·mol^{-1}).

https://doi.org/10.1021/acs.organomet.2c00018
Organometallics 2022, 41, 794−801

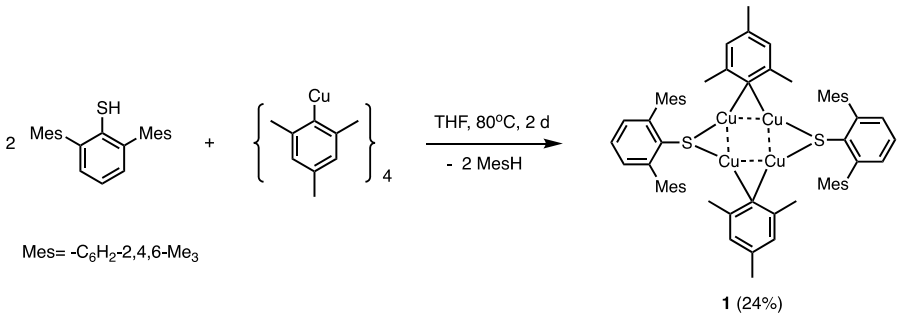

Figure 6. Synthesis of the complex **1**.

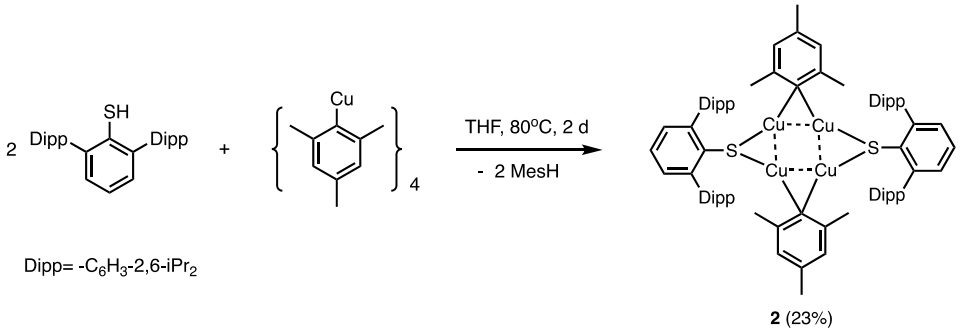

Figure 7. Synthesis of the complex **2**.

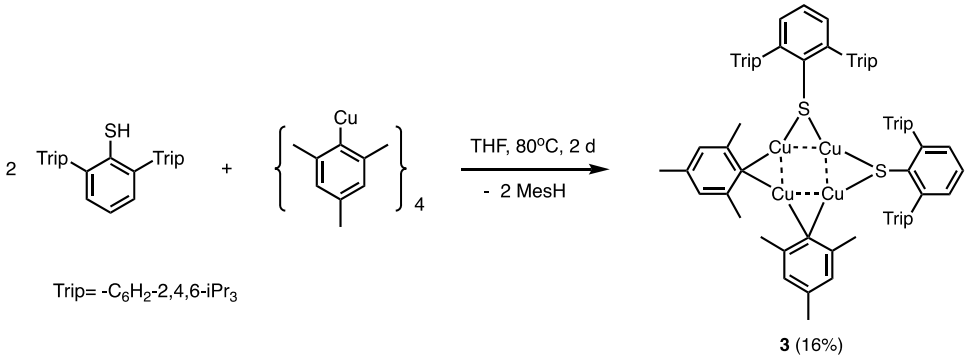

Figure 8. Synthesis of the complex **3**.

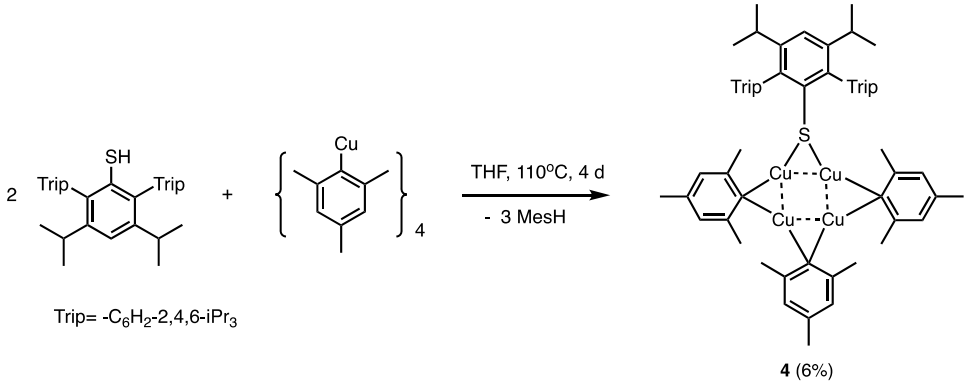

Figure 9. Synthesis of the complex **4**.

{Cu$_4$(SAr^{iPr8})Mes$_3$} (4). Complex **4** was prepared in a manner analogous to that used for complex **3**. HSAr^{iPr8} (0.4 g, 0.67 mmol) and {CuMes}$_4$ (0.243 g, 0.33 mmol) were combined as solids and ca. 50 mL of toluene was added, mixture was stirred at 110 °C for 4 days. The solvent was then removed under reduced pressure to afford an off-white residue. The residue was dissolved in ca. 50 mL of toluene, and the solvent was concentrated under reduced pressure to ca. 4 mL. The solution was then stored in a 5 °C refrigerator for 5 days to afford 0.11 g (6%) of product **4** as colorless blocks. mp 185−188 °C. ^{1}H NMR (600 MHz, benzene-d_6) δ 7.29 (d, J = 1.8 Hz, 1H), 7.08 (d, J = 1.9 Hz, 4H), 6.59 (s, 4H), 6.40 (s, 2H), 2.99 (td, J = 6.8, 2.0 Hz, 4H), 2.63 (d, J = 1.9 Hz, 12H), 2.55 (s, 2H), 2.51 (s, 6H), 2.44−2.39 (m,

https://doi.org/10.1021/acs.organomet.2c00018
Organometallics 2022, 41, 794−801

2H), 1.99 (d, J = 1.7 Hz, 6H), 1.83−1.76 (m, 12H), 1.76 (s, J = 1.7 Hz, 3H), 1.22 (dd, J = 7.0, 1.9 Hz, 12H), 1.07 (ddd, J = 13.4, 6.8, 1.9 Hz, 24H). ^{13}C NMR (150 MHz, benzene-d_6) δ 154.19, 153.28, 146.90, 145.68, 140.18, 136.69, 136.54, 135.58, 126.07, 125.91, 122.10, 32.32, 30.82, 30.32, 29.54, 28.53, 26.76, 24.67, 24.36, 23.03, 21.05, 20.92. UV−vis λ/nm (ε/M^{-1} cm^{-1}) 294 (2300). IR (Nujol; $\tilde{\nu}$/cm^{-1}) 1589w, 1518w, 1456s, 1372s, 1308w, 871w, 842w, 798w, 765w, 720w.

X-ray Crystallographic Studies. Crystals of complexes **1** and **2** suitable for X-ray crystallographic study were obtained from concentrated hexane solution at −18 °C after 4 to 5 days; **3** and **4** were recrystallized from concentrated toluene. Single crystals were removed from Schlenk tubes and immediately covered with a layer of hydrocarbon oil. Suitable crystals were selected, mounted on a nylon cryoloop, and then placed in the cold nitrogen stream of the diffractometer. Data for **1**−**4** were collected at 90(2) K with Cu Kα_1 radiation (λ = 1.5418 Å) using a Bruker DUO diffractometer in conjunction with a CCD detector. The collected reflections were corrected for Lorentz and polarization effects and for absorption by using Blessing's method as incorporated into the program SADABS.[28,29] The structures were solved by direct methods and refined with the SHELXTL (2012, version 6.1) or SHELXTL (2013) software packages.[30] Refinement was by full-matrix least-squares procedures, with all carbon-bound hydrogen atoms included in calculated positions and treated as riding atoms. The thermal ellipsoid plots were drawn using OLEX2 software.[31] A summary of the crystallographic and data collection parameters is given in Table S1 in the SI.

Computational Details. The geometry optimizations of both isomers **2** and **3** were performed with the Gaussian16 (Revision C.01) program[32] using the PBE1PBE hybrid exchange functional[33] and Def2-TZVP basis sets.[34] In addition, Grimme's empirical dispersion correction with Becke−Johnson damping (GD3BJ)[35] was used as well as an ultrafine integration grid. Full analytical frequency calculations were performed for the optimized structures to ensure the nature of the stationary points found (minima, no imaginary frequencies). The energy decomposition analyses (EDA)[36] were performed using ADF2021.102 program package.[37] These calculations utilized the PBE1PBE functional and TZ2P basis sets[38] for all atoms with empirical dispersion correction (GD3BJ) and good numerical quality.

■ ASSOCIATED CONTENT

Supporting Information

The Supporting Information is available free of charge at https://pubs.acs.org/doi/10.1021/acs.organomet.2c00018.

^{1}H and ^{13}C {^{1}H} spectra, crystallographic data, and details of computational studies (PDF)

Structure data (XYZ)

Accession Codes

CCDC 2129403−2129404 and 2129407−2129408 contain the supplementary crystallographic data for this paper. These data can be obtained free of charge via www.ccdc.cam.ac.uk/data_request/cif, or by emailing data_request@ccdc.cam.ac.uk, or by contacting The Cambridge Crystallographic Data Centre, 12 Union Road, Cambridge CB2 1EZ, UK; fax: +44 1223 336033.

■ AUTHOR INFORMATION

Corresponding Authors

Petra Vasko − *Department of Chemistry, University of Helsinki, FI-00014 Helsinki, Finland;* orcid.org/0000-0003-4202-6869; Email: petra.vasko@helsinki.fi

Philip P. Power − *Department of Chemistry, University of California, Davis, California 95616, United States;* orcid.org/0000-0002-6262-3209; Email: pppower@ucdavis.edu

Authors

Wenxing Zou − *Department of Chemistry, University of California, Davis, California 95616, United States*

James C. Fettinger − *Department of Chemistry, University of California, Davis, California 95616, United States;* orcid.org/0000-0002-6428-4909

Complete contact information is available at: https://pubs.acs.org/10.1021/acs.organomet.2c00018

Notes

The authors declare no competing financial interest.

■ ACKNOWLEDGMENTS

We thank the U.S. National Science Foundation for funding (Grant No. CHE-1565501) and for purchase of a dual source X-ray diffractometer (Grant No. CHE-0840444). PV would like to thank the Academy of Finland for funding (Project Numbers 314794, 338271, and 338271) and the CSC − IT Center for Science, Finland, for computational resources.

■ REFERENCES

(1) Bradley, D. C. Steric Control of Metal Coordination. *Chem. Br.* **1975**, *11*, 393−397.

(2) Power, P. P. Some Highlights from the Development and Use of Bulky Monodentate Ligands. *J. Organomet. Chem.* **2004**, *689*, 3904−3919.

(3) Lappert, M. F. Use of the Bulky Alkyl Ligand $(Me_3Si)_2CH$ to Stabilize Unusual Low Valent Transition Metal Alkyls and Dialkylstannylene Derivatives. *Adv. Chem.* **1976**, *150*, 256−265.

(4) Coles, M. P. the Role of the Bis-trimethylsilylamido Ligand, $[N\{SiMe_3\}_2]^-$, in Main Group Chemistry. Part 1: Structural Chemistry of the s-block Elements. *Coord. Chem. Rev.* **2015**, *297*−*298*, 2−23.

(5) Seidu, I.; Seth, M.; Ziegler, T. Role Played by Isopropyl Substituents in Stabilizing the Putative Triple Bond in Ar′EEAr′[E = Si, Ge, Sn; Ar′=C_6H_3-2,6(C_6H_3-2,6-Pri$_2$)$_2$] and Ar*PbPbAr* [Ar*=C_6H_3-2,6(C_6H_2-2,4,6-Pri$_3$)$_2$]. *Inorg. Chem.* **2013**, *52*, 8378−8388.

(6) Wagner, J. P.; Schreiner, P. R. London Dispersion in Molecular Chemistry-Reconsidering Steric Effects. *Angew. Chem., Int. Ed.* **2015**, *54*, 12274−12296.

(7) Pollard, V. A.; Kennedy, A. R.; McLellan, R.; Ross, D.; Tuttle, T.; Mulvey, R. E. Structurally Defined Ring-Opening and Insertion of Pinacolborane into Aluminium-Nitrogen Bonds of Sterically Demanding Dialkylaluminium Amides. *Eur. J. Inorg. Chem.* **2021**, *2021*, 50−53.

(8) Grimme, S.; Schreiner, P. R. Steric Crowding Can Stabilize a Labile Molecule: Solving the Hexaphenylethane Riddle. *Angew. Chem., Int. Ed.* **2011**, *50*, 12639−12642.

(9) Rekken, B. D.; Brown, T. M.; Fettinger, J. C.; Lips, F.; Tuononen, H. M.; Herber, R. H.; Power, P. P. Dispersion Forces and Counterintuitive Steric Effects in Main Group Molecules: Heavier Group 14 (Si-Pb) Dichalcogenolate Carbene Analogues with Sub-90° Interligand Bond Angles. *J. Am. Chem. Soc.* **2013**, *135*, 10134−10148.

(10) Liptrot, D. J.; Guo, J.; Nagase, S.; Power, P. P. Dispersion Forces, Disproportionation, and Stable High-Valent Late Transition Metal Alkyls. *Angew. Chem., Int. Ed.* **2016**, *55*, 14766−14769.

(11) Li, H.; Hu, Y.; Wan, D.; Zhang, Z.; Fan, Q.; King, R. B.; Schaefer, H. F. Dispersion Effects in Stabilizing Organometallic Compounds: Tetra-1-norbornyl Derivatives of the First-Row Transition Metals as Exceptional Examples. *J. Phys. Chem. A* **2019**, *123*, 9514−9519.

(12) Wagner, C. L.; Tao, L.; Thompson, E. J.; Stich, T. A.; Guo, J.; Fettinger, J. C.; Berben, L. A.; Britt, R. D.; Nagase, S.; Power, P. P. Dispersion-Force-Assisted Disproportionation: A Stable Two-Coor-

dinate Copper(II) Complex. *Angew. Chem., Int. Ed.* **2016**, *55*, 10444−10447.
(13) Zou, W.; Zhu, Q.; Fettinger, J. C.; Power, P. P. Dimeric Copper and Lithium Thiolates: Comparison of Copper Thiolates with Their Lithium Congeners. *Inorg. Chem.* **2021**, *60*, 17641−17648.
(14) Tsuda, T.; Yazawa, T.; Watanabe, K.; Fujii, T.; Saegusa, T. Preparation of Thermally Stable and Soluble Mesitylcopper(I) and its Application in Organic Synthesis. *J. Org. Chem.* **1981**, *46*, 192−194.
(15) Ito, M.; Hashizume, D.; Fukunaga, T.; Matsuo, T.; Tamao, K. Isolated Monomeric and Dimeric Mixed Diorganocuprates Based on the Size-Controllable Bulky "Rind" Ligands. *J. Am. Chem. Soc.* **2009**, *131*, 18024−18025.
(16) Li, B.; Zhang, C.; Yang, Y.; Zhu, H.; Roesky, H. W. Synthesis and Characterization of Heterobimetallic Al-O-Cu Complexes toward Models for Heterogeneous Catalysts on Metal Oxide Surfaces. *Inorg. Chem.* **2015**, *54*, 6641−6646.
(17) Pyykkö, P.; Atsumi, M. Molecular Single-Bond Covalent Radii for Elements 1−118. *Chem. Eur. J.* **2009**, *15*, 186−197.
(18) Tatewaki, H.; Hatano, Y.; Naka, T.; Noro, T.; Yamamoto, S. Atomic Radii for Depicting Atoms in a Molecule II: the Effective Atomic Radius and van der Waals Radius from ^{1}H to ^{54}Xe. *Bull. Chem. Soc. Jpn.* **2010**, *83*, 1203−1210.
(19) Dance, I. G.; Bowmaker, G. A.; Clark, G. R.; Seadon, J. K. the Formation and Crystal and Molecular Structures of Hexa(μ-organothiolato) Tetracuprate(I) Cage Dianions: Bis-(tetramethylammonium) Hexa(μ-methanethiolato)-Tetracuprate(I) and Two Polymorphs of Bis(tetramethylammonium) hexa(μ-benzenethiolato)-Tetracuprate(I). *Polyhedron* **1983**, *2*, 1031−1043.
(20) Stollenz, M.; Meyer, F. Mesitylcopper-A Powerful Tool in Synthetic Chemistry. *Organometallics* **2012**, *31*, 7708−7727.
(21) Rungthanaphatsophon, P.; Barnes, C. L.; Walensky, J. R. Copper(I) Clusters with Bulky Dithiocarboxylate, Thiolate, and Selenolate Ligands. *Dalton Trans.* **2016**, *45*, 14265−14276.
(22) Satyachand Harisomayajula, N. V.; Wu, B.-H.; Lu, D.-Y.; Kuo, T.-S.; Chen, I.-C.; Tsai, Y.-C. Ligand-Unsupported Cuprophilicityin the Preparation of Dodecacopper(I) Complexes and Raman Studies. *Angew. Chem., Int. Ed.* **2018**, *57*, 9925−9929.
(23) Satyachand Harisomayajula, N. V.; Makovetskyi, S.; Tsai, Y.-C. Cuprophilic Interactions in and between Molecular Entities. *Chem. Eur. J.* **2019**, *25*, 8936−8954.
(24) Chiarella, G. M.; Melgarejo, D. Y.; Rozanski, A.; Hempte, P.; Perez, L. M.; Reber, C.; Fackler, J. P., Jr. A Short, Unsupported Cu(I)–Cu(I) interaction, 2.65 Å, in A Dinuclear Guanidine Chloride Complex. *Chem. Commun.* **2010**, *46*, 136−138.
(25) Pratt, J.; Bryan, A. M.; Faust, M.; Boynton, J. N.; Vasko, P.; Rekken, B. D.; Mansikkamaki, A.; Fettinger, J. C.; Tuononen, H. M.; Power, P. P. Effects of Remote Ligand Substituents on the Structures, Spectroscopic, and Magnetic Properties of Two-Coordinate Transition-Metal Thiolate Complexes. *Inorg. Chem.* **2018**, *57*, 6491−6502.
(26) Pangborn, A. B.; Giardello, M. A.; Grubbs, R. H.; Rosen, R. K.; Timmers, F. J. Safe and Convenient Procedure for Solvent Purification. *Organometallics* **1996**, *15*, 1518−1520.
(27) Barnett, B. R.; Mokhtarzadeh, C. C.; Lummis, P.; Wang, S.; Queen, J. D.; Gavenonis, J.; Schüwer, N.; Tilley, T. D.; Boynton, J. N.; Power, P. P.; Ditri, T. B.; Weidemann, N.; Agnew, D. W.; Figueroa, J. S.; Smith, P. W.; Carpenter, A. E.; Pratt, J. K.; Mendelson, N. D.; Figueroa, J. S. Terphenyl Ligands and Complexes. *Inorg. Synth.* **2018**, *37*, 85−122.
(28) Sheldrick, G. M. *SADABS, Siemens Area Detector Absorption Correction*; Göttingen Universitaẗ: Göttingen, Germany, 2008; p 33.
(29) Blessing, R. H. An Empirical Correction for Absorption Anisotropy. *Acta Cryst. Sect. A: Found. Cryst.* **1995**, *51*, 33−38.
(30) Sheldrick, G. M. *SHELXTL*, Ver. 6.1; Bruker AXS: Madison, WI, 2002.
(31) Dolomanov, O. V.; Bourhis, L. J.; Gildea, R. J.; Howard, J. A. K.; Puschmann, H. OLEX2: A Complete Structure Solution, Refinement and Analysis Program. *J. Appl. Crystallogr.* **2009**, *42*, 339−341.
(32) Frisch, M. J.; Trucks, G. W.; Schlegel, H. B.; Scuseria, G. E.; Robb, M. A.; Cheeseman, J. R.; Scalmani, G.; Barone, V.; Petersson, G. A.; Nakatsuji, H.; Li, X.; Caricato, M.; Marenich, A. V.; Bloino, J.; Janesko, B. G.; Gomperts, R.; Mennucci, B.; Hratchian, H. P.; Ortiz, J. V.; Izmaylov, A. F.; Sonnenberg, J. L.; Williams-Young, D.; Ding, F.; Lipparini, F.; Egidi, F.; Goings, J.; Peng, B.; Petrone, A.; Henderson, T.; Ranasinghe, D.; Zakrzewski, V. G.; Gao, J.; Rega, N.; Zheng, G.; Liang, W.; Hada, M.; Ehara, M.; Toyota, K.; Fukuda, R.; Hasegawa, J.; Ishida, M.; Nakajima, T.; Honda, Y.; Kitao, O.; Nakai, H.; Vreven, T.; Throssell, K.; Montgomery, J. A.; Peralta, J. E., Jr.; Ogliaro, F.; Bearpark, M. J.; Heyd, J. J.; Brothers, E. N.; Kudin, K. N.; Staroverov, V. N.; Keith, T. A.; Kobayashi, R.; Normand, J.; Raghavachari, K.; Rendell, A. P.; Burant, J. C.; Iyengar, S. S.; Tomasi, J.; Cossi, M.; Millam, J. M.; Klene, M.; Adamo, C.; Cammi, R.; Ochterski, J. W.; Martin, R. L.; Morokuma, K.; Farkas, O.; Foresman, J. B.; Fox, D. J. *Gaussian 16*, Revision C.01; Gaussian, Inc.: Wallingford, CT, 2019.
(33) (a) Perdew, J. P.; Burke, K.; Ernzerhof, M. Generalized Gradient Approximation Made Simple. *Phys. Rev. Lett.* **1996**, *77*, 3865−3868. (b) Perdew, J. P.; Burke, K.; Ernzerhof, M. Generalized Gradient Approximation Made Simple. *Phys. Rev. Lett.* **1997**, *78*, 1396−1396. (c) Adamo, C.; Barone, V. Toward Reliable Density Functional Methods without Adjustable Parameters: the PBE0Model. *J. Chem. Phys.* **1999**, *110*, 6158−6169.
(34) (a) Weigend, F.; Ahlrichs, R. Balanced Basis Sets of Split Valence, Triple Zeta Valence and Quadruple Zeta Valence Quality for H to Rn: Design and Assessment of Accuracy. *Phys. Chem. Chem. Phys.* **2005**, *7*, 3297−3305. (b) Weigend, F. Accurate Coulomb-Fitting Basis Sets for H to Rn. *Phys. Chem. Chem. Phys.* **2006**, *8*, 1057−1065.
(35) Grimme, S.; Ehrlich, S.; Goerigk, L. Effect of the Damping Function in Dispersion Corrected Density Functional Theory. *J. Comput. Chem.* **2011**, *32*, 1456−1465.
(36) (a) Rodríguez, J. I.; Bader, R. F. W.; Ayers, P. W.; Michel, C.; Götz, A. W.; Bo, C. A High Performance Grid-Based Algorithm for Computing QTAIM Properties. *Chem. Phys. Lett.* **2009**, *472*, 149−152. (b) Rodríguez, J. I. An Efficient Method for Computing the QTAIM Topology of A Scalar Field: the Electron Density Case. *J. Comput. Chem.* **2013**, *34*, 681−686.
(37) (a) Te Velde, G.; Bickelhaupt, F. M.; Baerends, E. J.; Fonseca Guerra, C.; van Gisbergen, S. J. A.; Snijders, J. G.; Ziegler, T. Chemistry with ADF. *J. Comput. Chem.* **2001**, *22*, 931−967. (b) *ADF 2021.1, SCM, Theoretical Chemistry*; Vrije Universiteit: Amsterdam, The Netherlands. http://www.scm.com.
(38) van Lenthe, E.; Baerends, E. J. Optimized Slater-type Basis Sets for the Elements 1−118. *J. Comput. Chem.* **2003**, *24*, 1142−1156.

https://doi.org/10.1021/acs.organomet.2c00018
Organometallics 2022, 41, 794−801